Geophysical Research Letters

RESEARCH LETTER
10.1029/2024GL110491

Shifts in Maritime Trade Routes as a Result of Red Sea Shipping Crisis Detected in TROPOMI NO_2 Data

A. Pseftogkas[1], T. Stavrakou[2], J.-F. Müller[2], M.-E. Koukouli[1], D. Balis[1], and C. Meleti[1]

[1]Laboratory of Atmospheric Physics, Aristotle University of Thessaloniki, Thessaloniki, Greece, [2]Royal Belgian Institute for Space Aeronomy (BIRA-IASB), Brussels, Belgium

Key Points:

- Red Sea ship attacks have shifted international maritime trade routes
- NO_2 shipping levels decline by 55% in the Red Sea, 15% in the Gibraltar Strait, and increase by 40% off the coast of South Africa
- NO_2 shipping trends correspond to changes in the number of vessels

Correspondence to:

A. Pseftogkas,
anpsefto@auth.gr

Citation:

Pseftogkas, A., Stavrakou, T., Müller, J.-F., Koukouli, M.-E., Balis, D., & Meleti, C. (2024). Shifts in maritime trade routes as a result of Red Sea shipping crisis detected in TROPOMI NO_2 data. *Geophysical Research Letters*, *51*, e2024GL110491. https://doi.org/10.1029/2024GL110491

Received 31 MAY 2024
Accepted 7 OCT 2024

Abstract Observations from space-borne spectrometers have been lately used to quantify shipping emissions of nitrogen oxides (NO_X). Here we present a method that enhances the shipping signal of NO_2 TROPOspheric MOnitoring Instrument (TROPOMI) satellite sensor observations in order to assess the impact of the Red Sea ship attacks on NO_2 levels in three important shipping routes along the Red Sea, the Cape of Good Hope, and the Gibraltar Strait. Major shipping carriers, sailing usually via the Red Sea, have responded to the attacks by transiting their fleet around the African continent. The shipping signal from TROPOMI declines by ∼55% in the Red Sea and ∼15% in the Gibraltar Strait while an increase of ∼40% is found off the South African coast between January–June 2024 and the same period in 2023. These changes correlate well with vessel statistics, demonstrating the ability to track abrupt changes in NO_2 shipping levels with satellite measurements.

Plain Language Summary Since the beginning of the Red Sea attacks on commercial vessels in late 2023, trade operations have been disrupted and international maritime routes have shifted away from the Red Sea. We use satellite measurements of atmospheric pollutants, capable of detecting emissions from ships along main trade routes, in order to examine the impact of the attacks along busy shipping lanes in the Red Sea, off the coast of South Africa and the Gibraltar Strait. Air pollution levels from ships show reductions of 55% and 15% in the Red Sea and Gibraltar areas, respectively, and an increase of 40% off the coast of South Africa, in the aftermath of the attacks. Changes in air pollution levels are well in line with changes in the number of ships transiting through these areas. Ship presence declined by approximately 55% and 15% in the Red Sea and the Gibraltar Strait, whereas it increased by 80% off the coast of South Africa. Both satellite observations and ship numbers verify quantitatively the re-routing of ships away from the Red Sea through the coast of South Africa.

1. Introduction

The maritime sector is responsible for the transportation of approximately 80% of global goods (UNCTAD, 2022), and is one of the most vital components of global economy (Schnurr & Walker, 2019). Since human activities and global economy are closely related to anthropogenic emissions of trace gases in the atmosphere (Raupach et al., 2007), an increase in maritime sector emissions by 90% is expected by 2050 compared to the global economic recession levels of 2008 (Faber et al., 2020). Shipping activities are responsible for emissions of hazardous pollutants such as nitrogen oxides ($NO_X = NO_2 + NO$), sulfur oxides (SO_X), carbon monoxide (CO) and particulate matter (PM) with severe implications for human health and the environment (Eyring et al., 2010; Smith et al., 2014). Recent studies have shown that international shipping accounts for 15%–35% of total anthropogenic NO_X emissions (Crippa et al., 2018), and for ca. 3% of global greenhouse emissions (IPCC, 2022). In this context, the International Maritime Organization (IMO) has proceeded to the implementation of mitigation strategies by reducing the sulfur content in ship fuels in specific marine Emission Control Areas (ECAs) (IMO MARPOL ANNEX VI–Regulation 13, 2020). Many marine areas are still not designated as ECAs and a close monitoring of shipping emissions is therefore required.

Space-borne measurements of nitrogen dioxide (NO_2) have been employed to assist in the monitoring of NO_2 shipping signal from space. In the past years, satellite measurements of NO_2 column densities from various sensors have been utilized to detect NO_2 levels along major international shipping lanes (Beirle et al., 2004; Marmer et al., 2009; Richter, 2009; Vinken et al., 2014) and to provide quantative information on NO_2 shipping emissions. Furthermore, de Ruyter de Wildt et al. (2012) estimated NO_2 shipping satellite-derived signals and identified common trends between the NO_2 shipping signal and global trade economic data. Thanks to the enhanced spatial resolution of the TROPOMI instrument (3.5 km × 5.5 km, Veefkind et al., 2012), the detection

of NO_2 emissions from individual ships was shown to be feasible (Ding et al., 2020; Georgoulias et al., 2020; Kurchaba et al., 2024). The impact of the COVID-19 pandemic on NO_X shipping emissions as sensed by TROPOMI in European seas (Riess et al., 2022), demonstrated that satellite measurements can detect abrupt changes in shipping activity.

In this study, we utilize the NO_2 tropospheric vertical column measurements from TROPOMI to assess the impact of the Red Sea attacks on ship traffic and associated NO_x emissions along major international shipping lanes. The Israel-Hamas conflict has triggered attacks on commercial vessels in the Gulf of Aden by the Yemen-based Houthi movement, disrupting trade operations and leading to the re-routing of vessels away from the Red Sea through the Cape of Good Hope, off the coast of South Africa. Our method follows Latsch et al. (2022) and aims to strengthen the weak NO_2 satellite shipping signal and derive non-linear trends of NO_2 over the shipping lanes south of the Suez Canal and through the Straits of Bab el-Mandeb (a narrow passage connecting the Red Sea to the Gulf of Aden), the Cape of Good Hope and Gibraltar. This method tentatively subtracts the background NO_2 levels and the outflow from continental emissions, in order to highlight the NO_2 signal over shipping routes in background and in polluted areas. We further associate the changes in the NO_2 satellite-derived shipping signal with shipping activity statistics in the target regions.

2. Satellite Data and Methodology

We use the reprocessed v.02.04.00. S5P/TROPOMI NO_2 tropospheric vertical column densities (TVCDs, van Geffen et al., 2022) over the areas of interest for the period between January 2019 and June 2024. Satellite data are binned onto a $0.05° \times 0.1°$ grid before implementing the shipping signal enhancement methodology. Only satellite pixels with a quality assurance value higher than 0.75 are selected, corresponding to a cloud fraction below 0.5 (van Geffen et al., 2022). Measurements are obtained on a daily basis in the early afternoon (approximately 13:30 local time), when NO_2 levels exhibit lower values in the daily cycle, due to photolysis. Nevertheless, shipping signal is visible over pristine marine areas overlain by the most traveled shipping routes, because NO_X has a relatively short lifetime and is detected close to the emission source.

Figure 1 (left) shows the average NO_2 TVCDs for the period between January–June 2019-2023, measured by TROPOMI over the Red Sea, the Cape of Good Hope and the Gibraltar Strait regions, and the average relative differences (right) between January–June 2024 and the same period in 2019–2023. The shipping signal from the satellite is visible in all three regions, confined in narrow and well-defined shipping lanes. A clear shipping track in the Levantine Sea leading to the Suez Canal crossing the Red Sea and the Bab el-Mandeb Strait, stretches down to the Gulf of Aden. Off the coast of South Africa, a well defined NO_2 shipping signal can be detected between Port Elizabeth and the Port of Cape Town, whereas in the Gibraltar Strait, the satellite detects the shipping signal crossing into the Mediterranean Sea. The effect of the Red Sea ship attacks is imprinted in the relative differences for each selected region.

The method for estimating changes in the shipping signal of satellite observations, while accounting for background values, was initially implemented by de Ruyter de Wildt et al. (2012). Over marine pristine shipping lanes, NO_2 total tropospheric column abundances ($TVCD_{tot}$) are composed of the shipping signal ($TVCD_{ship}$) and the background NO_2 levels ($TVCD_{bg}$) of the adjacent regions not affected by shipping emissions. Small fluctuations in the background signal are attributed mainly to variations in meteorology and satellite position. Hence, over a given shipping lane, $TVCD_{ship}$, that is, the clean shipping signal, is estimated by subtracting the background levels of the adjacent regions from the total NO_2 levels. The limitation of this method lies in the estimation of $TVCD_{ship}$ over areas affected by the outflow of inland emissions. In those cases, the outflow component ($TVCD_{out}$) of the total NO_2 TVCDs needs to be quantified, but its estimation is made difficult due to the overlap between the different contributions near coastlines.

To overcome this shortcoming, an alternative filtering method is implemented in this study to account for the impact of the land-based emissions outflow (Latsch et al., 2022). We first estimate the monthly averages for each studied region to minimize short-term variations and then proceed with the implementation of the filtering method to highlight the shipping signal. Specifically, an average of neighboring pixels within a grid box of $1° \times 1°$ is subtracted from the original pixel value of every single grid cell (with size of $0.05° \times 0.1°$) over land and sea of the predefined domain. NO_2 TVCDs over land are, finally, masked after the application of the filtering to focus solely on the shipping signal. The choice of the size of the larger grid box ($1° \times 1°$) has been made after different tests with variable grid box sizes. Over land, it ensures the detection of emission hotspots and accounts

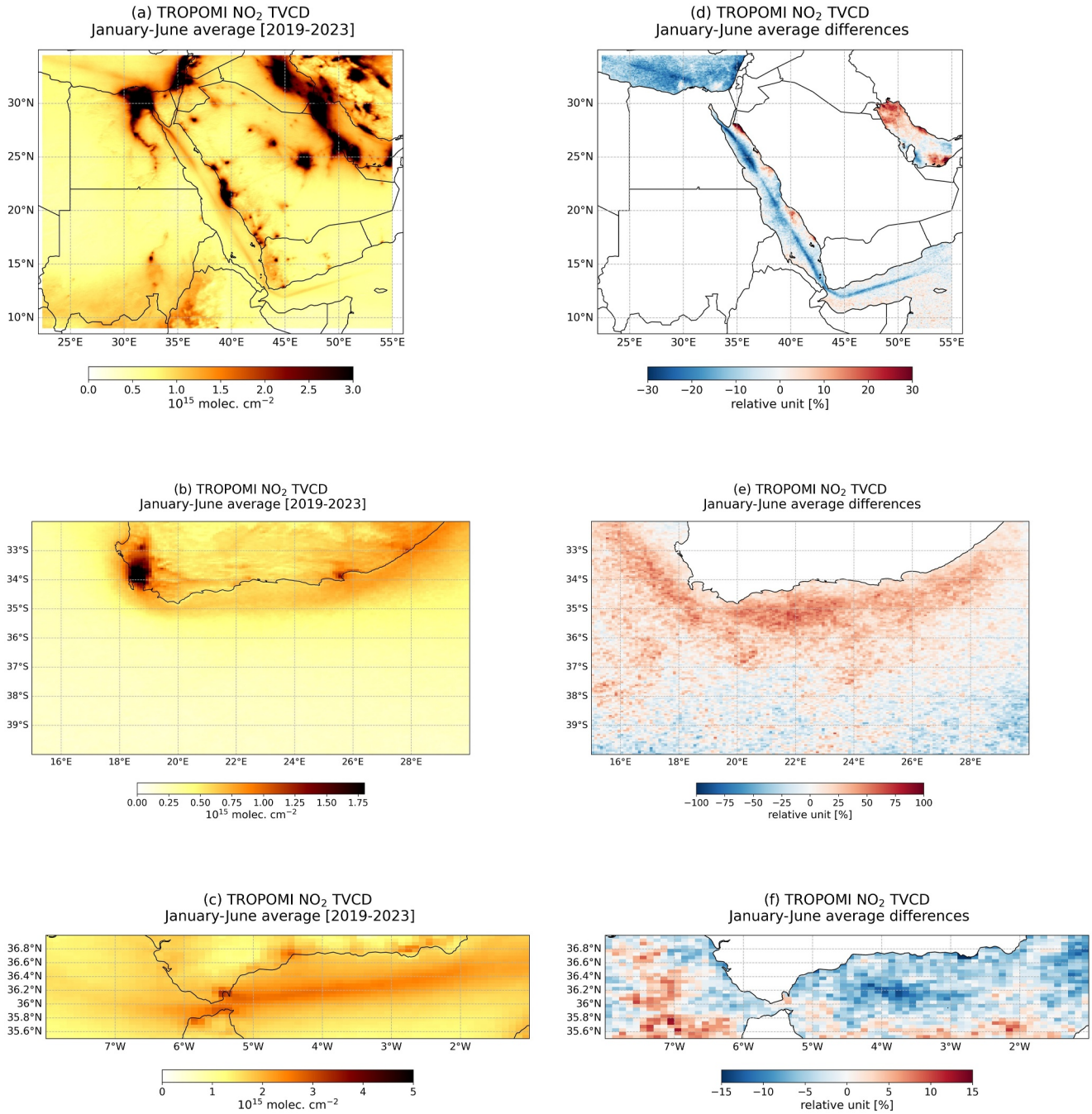

Figure 1. NO_2 mean TVCDs (10^{15} molec. cm^{-2}) detected by TROPOMI for the period January–June 2019-2023 over (a) the Red Sea, (b) the South African coastline and (c) the Gibraltar Strait. NO_2 TVCDs mean relative differences between the period January-June 2024 and January-June 2019-2023 over (d) the Red Sea, (b) the South Africa coastline and (c) the Gibraltar Strait. NO_2 TVCDs over land are masked.

for the outflow of emissions on shipping lanes in the vicinity of land-based emitting sources. Hence, this method highlights successfully the shipping signal, limiting the striping structures in subtropical regions.

3. Results

3.1. NO_2 Shipping Signal and Vessel Statistics

A demonstration of the NO_2 shipping signal derivation described above is shown in Figure 2, for the January-June period of 2023 (left) and 2024 (right). Here, well-structured shipping routes are identified in all regions after

10.1029/2024GL110491

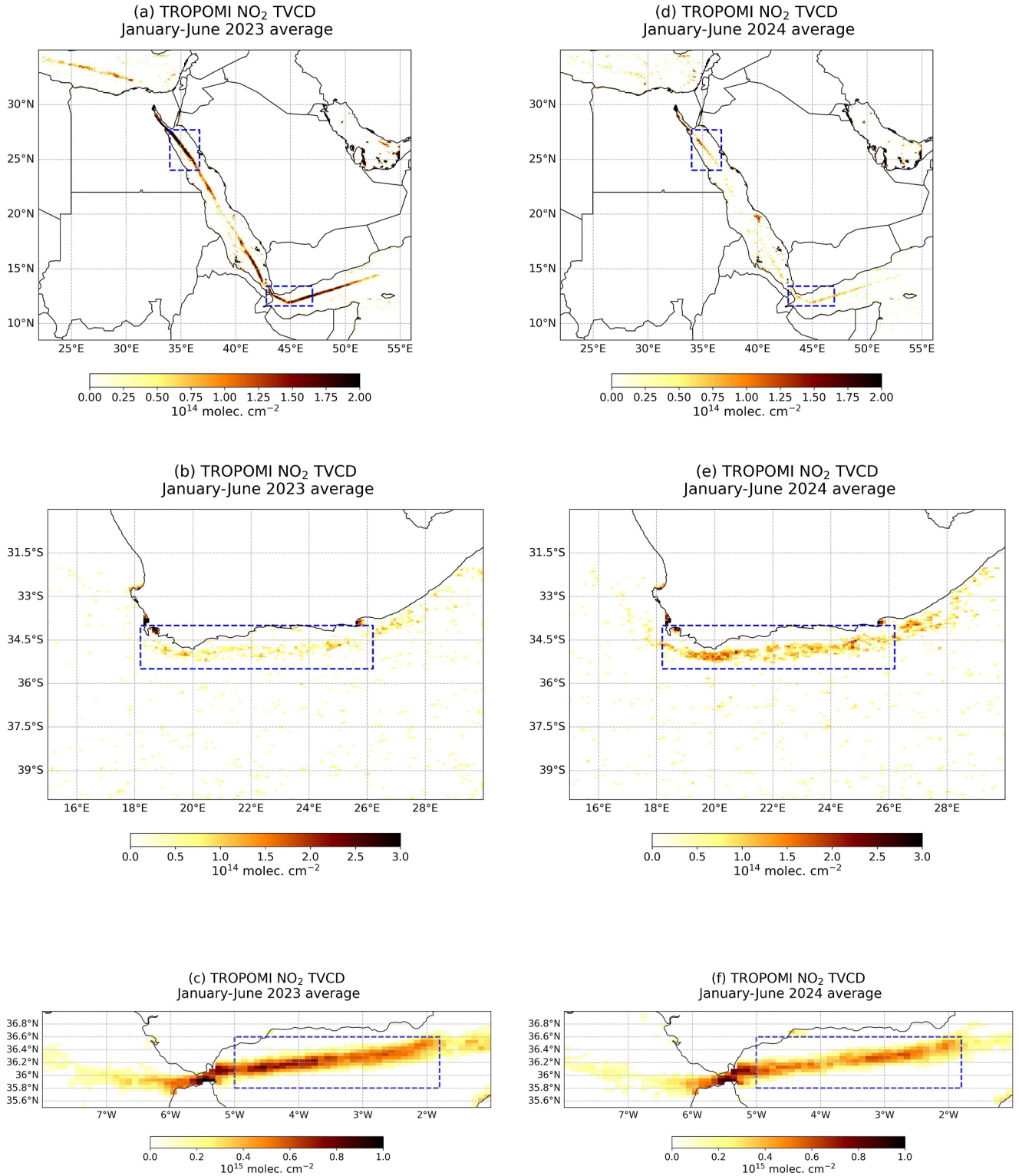

Figure 2. NO_2 shipping signal (molec. cm^{-2}) for the January-June period of 2023 (left) and 2024 (right) over the (a), (d) Red Sea (b), (e) South African coastline and (c), (f) Gibraltar Strait. Blue boxes indicate the parts of the examined shipping tracks.

accounting for the background and outflow segregation. NO_2 levels are overall low (order of 10^{14} molec. cm^{-2}) for the Red Sea and South Africa regions and an order of magnitude higher in the Gibraltar Strait. Significant changes are observed in the Red Sea, where NO_2 TVCDs are lower in January-June 2024 by approximately 55% across the whole shipping track. Off the South African Coast, NO_2 TVCDs display an enhancement of ∼40%. Differences are less pronounced in the Gibraltar Strait but still visible. NO_2 TVCDs are lower by ∼15% compared to January-June 2023 levels.

To better quantify the impact of the Red Sea crisis on NO_2 shipping levels and to associate them with changes in vessel activity, we focus on parts of shipping lanes in the proximity of high-density maritime gateways, delimited by the blue boxes in Figure 2. Namely, the satellite-derived shipping signal is examined near the Suez Canal, the Bab el-Mandeb Strait, the Cape of Good Hope and the Gibraltar Strait. Vessel data are acquired from the International Monetary Fund-PortWatch platform (IMF-PortWatch, https://portwatch.imf.org/, last accessed on 30 August 2024), which monitors trade disruptions from natural disasters and unforeseen events. PortWatch uses AIS (Automatic Identification System) satellite-based vessel data to track the number of vessels operating in international ports and maritime gateways. In this work, we take advantage of the publicly available beta version that allows users to acquire vessel and trade data in various locations. We aggregate the daily number of vessels operated in the Suez Canal, the Bab el-Mandeb Strait, the Cape of Good Hope and the Gibraltar Strait into monthly totals and compare the ship data variations with the NO_2 satellite-derived shipping signal monthly fluctuations over the four defined shipping lanes in the vicinity of the maritime gateways.

Figure 3 shows the monthly variations of the NO_2 shipping signal compared with the total monthly number of ships crossing through the four examined regions between January 2019 and June 2024. Because NO_2 has a seasonal variability, with highs in winter and lows in summer due to higher photolysis rates and photochemical activity in summer, we remove this seasonality from the NO_2 timeseries to achieve a more realistic comparison with the ship data. This is done by decomposing the timeseries into three components (trend, seasonality, residual) within a 12 month window. The decomposition assumes a multiplicative relationship between the three components and the seasonal patterns are removed by dividing the original values by the seasonal component. The shaded area in Figure 3 shows the uncertainty in the estimation of the shipping signal based on the application of the filtering method to the daily NO_2 TVCDs distributions and the calculation of the standard deviations of the resulting fields, after the removal of the seasonal component.

Overall, the de-seasonalized monthly satellite-derived NO_2 shipping signal demonstrates a strong temporal correlation (∼0.78) in the Suez Canal, the Bab el-Mandeb Strait (∼0.85) and the Cape of Good Hope Strait (∼0.73) with the total number of vessels, and a moderate correlation (∼0.5) over the Gibraltar Strait. Specifically, over the Suez Canal, the monthly number of vessels steadily increased from January 2019 (∼1,500 vessels) to November 2023 (∼2,500 vessels) and after the recent attacks showed a sharp decrease to unprecedented levels (∼1,000 vessels in March 2024) in this 6 year span. This pattern is also well captured by the satellite data, with the NO_2 shipping signal reporting the lowest values (∼0.5 × 10^{14} molec. cm^{-2}) in the aftermath of the attacks. Both the NO_2 shipping signal and the number of vessels slightly declined afterward, until June 2024. Similar variations in both ship data and NO_2 shipping signal are also observed in the Bab el-Mandeb Strait, with the number of ships (<1,000) and NO_2 levels (<0.5 × 10^{14} molec. cm^{-2}) reaching their lowest values in May 2024. Off the South African coast, the alternative route used by ships to avoid the Red Sea route, both the number of vessels (1,300–1,700 vessels) and the NO_2 shipping signal (0.6–0.8 × 10^{14} molec. cm^{-2}) are very stable from January 2019 until December 2023. In January 2024, more than 2200 ships passed through the Cape of Good Hope, equivalent to a ∼45% increase compared to the period between January 2019-December 2023, whereas a ∼40% increase in the NO_2 shipping signal was observed along the shipping lane (Figure 2). The number of vessels further increased until June 2024, whereas the shipping signal also increased, except for a small drop in February 2024. Finally, over the Gibraltar Strait, the connective link between the Mediterranean and the Red Sea shipping routes, NO_2-derived shipping levels and vessel numbers displayed a slight increasing trend until November 2023, and a drop afterward until February 2024 by ∼30%, compared to November 2023 levels. In March 2024, both vessel numbers and NO_2 levels showed a slight increase, followed by a declining trend until June 2024, when both the NO_2 shipping signal and the number of vessels reported the lowest values in 2024. Overall, the Red Sea crisis has resulted in a 15% decrease of both NO_2 shipping levels and vessel numbers in January-June 2024 compared to 2023 levels. This lesser impact across the Gibraltar Strait

Figure 3. Monthly NO_2 satellite-derived shipping signal (10^{14} molec. cm^{-2}), after the removal of seasonal variability, over the Suez Canal, Bab el-Mandeb Strait, South Africa and Gibraltar Strait shipping areas defined in Figure 2, compared with the corresponding total monthly number of vessels (gray). The shaded blue areas show the uncertainty estimates of the NO_2 shipping signal. In the top right corner, the temporal correlation coefficient (blue) between the NO_2 shipping signal and the number of vessels is shown.

compared to the Red Sea could be explained by the large proportion of ships from the Cape of Good Hope unloading their cargo in Western Mediterranean ports such as Barcelona and Tangiers, before continuing their route toward Northern Europe (Bouissou et al., 2024). A detailed overview of the relative changes in the number of vessels and NO_2 shipping levels between the periods of January-June 2024, January-June 2019-2023 and January-June 2023 is given in Table 1. The period of January-June is selected as it is seemingly the most impacted in the aftermath of the Red Sea crisis.

Table 1
Relative Percentage Differences and Their Uncertainty Estimates Between the January-June 2024 Average and Either the Corresponding 2019–2023 Average or the Corresponding 2023 Average of the NO_2 Satellite-Derived Shipping Signal and of the Number of Vessels in the Examined Regions

Region	NO_2 change relative to 2019–2023	Vessels change relative to 2019–2023	NO_2 change relative to 2023	Vessels change relative to 2023
Suez Canal	−52 ± 24%	−38%	−56 ± 22%	−50%
Bab el-Mandeb Strait	−51 ± 18%	−51%	−56 ± 17%	−60%
South Africa	+46 ± 39%	+77%	+37 ± 38%	+78%
Gibraltar	−9 ± 44%	−4%	−16 ± 43%	−14%

4. Conclusions

The impact of the Red Sea crisis on NO_2 levels along one of the main trade routes between Asia, Middle East and Europe (ca. 12% of the world trade) was detected in the TROPOMI NO_2 TVCD measurements. To identify underlying trends in NO_2 shipping levels, over pristine and polluted areas, where NO_2 shipping signal intermingles with continental emissions, a method that enhances the shipping signal is implemented. Monthly variations of NO_2 shipping levels and vessel numbers are examined for a 6 year period (January 2019-June 2024) over the Suez Canal, the Bab el-Mandeb Strait, the Cape of Good Hope and the Gibraltar Strait regions. Observations suggest a reduction of ∼55% on both the NO_2 satellite-derived shipping signal and the number of vessels in the Suez Canal and the Bab el-Mandeb Strait in January-June 2024. On the contrary, ship presence has increased by ∼80% in the Cape of Good Hope, accompanied by a ∼40% increase of NO_2 satellite-derived shipping levels off the coast of South Africa. The effect on the Gibraltar Strait NO_2 shipping signal is less pronounced, due to vessels coming from Cape of Good Hope unloading their cargo in Western Mediterranean ports, but not insignificant. Vessels and NO_2 shipping level estimates decrease by 15% in January-June 2024 compared to January-June 2023 levels, reflecting the impact of the ongoing Red Sea crisis on high-density maritime gateways.

To conclude, we presented an effective way to highlight the NO_2 shipping signal over major international shipping lanes. The good agreement in the temporal variations between the NO_2 satellite-derived shipping signal and shipping activity suggests that the background and outflow signals have been largely accounted for. Hence, shifts in the maritime commercial routes can be detected by changes in NO_2 shipping emissions observed by space-borne instruments.

Conflict of Interest

The authors declare no conflicts of interest relevant to this study.

Data Availability Statement

The S5P/TROPOMI NO_2 observations are stored in the Copernicus Data Space Ecosystem platform (https://dataspace.copernicus.eu/, last accessed on 30 August 2024) and are publicly available via the dataset landing page: https://t.ly/N1Wlx (last accessed on 30 August 2024, a free registration is required). Vessel statistics from the beta version of the IMF PortWatch platform are stored online (https://portwatch.imf.org/, last accessed on 30 August 2024). The Gibraltar Strait dataset landing page is: https://portwatch.imf.org/pages/d2b71882a70449288ee9bd15421d2aa9 (last accessed on 30 August 2024) and the Red Sea-Cape of Good Hope dataset landing page is: https://portwatch.imf.org/pages/573013af3b6545deaeb50ed1cbaf9444 (last accessed on 30 August 2024).

Acknowledgments

This research has been co-financed by the European Union (European Regional Development Fund) and Greek national funds through the Operational Program "Competitiveness, Entrepreneurship and Innovation" (NSRF 2014–2020) and co-financed by the Hellenic Foundation for Research and Innovation (HFRI) under the third Call for HFRI PhD Fellowships (Fellowship Number: 5907). Results presented in this work have been produced using the Aristotle University of Thessaloniki (AUTH) High Performance Computing Infrastructure and Resources. The authors would like to acknowledge the support provided by the AUTH IT Centre throughout the progress of this research work. We further acknowledge the Atmospheric Toolbox®. T.S. would like to acknowledge support by the Belgian Science Policy Office through the PRODEX TROVA-E2 project.

References

Beirle, S., Platt, U., von Glasow, R., Wenig, M., & Wagner, T. (2004). Estimate of nitrogen oxide emissions from shipping by satellite remote sensing. *Geophysical Research Letters*, *31*(18), L18102. https://doi.org/10.1029/2004GL020312

Bouissou, J., Morel, S., & Rafenberg, M. (2024). La crise en mer Rouge dérègle le transport maritime. *Le Monde*. https://www.lemonde.fr/economie/article/2024/05/17/commerce-mondial-la-crise-en-mer-rouge-deregle-le-transport-maritime_6233760_3234.html

Crippa, M., Guizzardi, D., Muntean, M., Schaaf, E., Dentener, F., van Aardenne, J. A., et al. (2018). Gridded emissions of air pollutants for the period 1970–2012 within EDGAR v4.3.2. *Earth System Science Data*, *10*(4), 1987–2013. https://doi.org/10.5194/essd-10-1987-2018

de Ruyter de Wildt, M., Eskes, H., & Boersma, K. F. (2012). The global economic cycle and satellite-derived NO_2 trends over shipping lanes. *Geophysical Research Letters*, *39*(1), L01802. https://doi.org/10.1029/2011GL049541

Ding, J., vander A, R. J., Eskes, H. J., Mijling, B., Stavrakou, T., van Geffen, J. H. G. M., et al. (2020). NOx emissions reduction and rebound in China due to the COVID-19 crisis. *Geophysical Research Letters*, *46*, e2020GL089912. https://doi.org/10.1029/2020GL089912

Eyring, V., Isaksen, I. S. A., Berntsen, T., Collins, W. J., Corbett, J. J., Endresen, Ø., et al. (2010). Transport impacts on atmosphere and climate: Shipping. *Atmospheric Environment*, *44*(37), 4735–4771. https://doi.org/10.1016/j.atmosenv.2009.04.059

Faber, J., Hanayama, S., Zhang, S., Pereda, P., Comer, B., Hauerhof, E., et al. (2020). *Fourth IMO greenhouse gas study*. International Maritime Organization (IMO). Retrieved from https://docs.imo.org (last accessed on May 22, 2024)

Georgoulias, A. K., Boersma, K. F., Van Vliet, J., Zhang, X., Van Der A, R., Zanis, P., & De Laat, J. (2020). Detection of NO_2 pollution plumes from individual ships with the TROPOMI/S5P satellite sensor. *Environmental Research Letters*, *15*(12), 124037. https://doi.org/10.1088/1748-9326/abc445

IMF PortWatch platform vessel data. UN global platform and IMF PortWatch (Retrieved from portwatch.imf.org, last accessed on May 22, 2024).

IMO MARPOL ANNEX. VI – Regulation 13 2020. Retrieved from https://www.imo.org/es/OurWork/Environment/Pages/Index-of-MEPC-Resolutions-and-Guidelines-related-to-MARPOL-Annex-VI.aspx (last accessed on May 22, 2024).

IPCC. (2022). In P. R. Shukla, J. Skea, R. Slade, A. Al Khourdajie, R. van Diemen, et al. (Eds.), *Climate change 2022: Mitigation of climate change. Contribution of working group III to the sixth assessment report of the intergovernmental panel on climate change*. Cambridge University Press. https://doi.org/10.1017/9781009157926

Kurchaba, S., Sokolovsky, A., van Vliet, J., Verbeek, F. J., & Veenman, C. J. (2024). Sensitivity analysis for the detection of NO_2 plumes from seagoing ships using TROPOMI data. *Remote Sensing of Environment*, *304*, 114041. https://doi.org/10.1016/j.rse.2024.114041

Latsch, M., Richter, A., Lange, K., & Burrows, J. P. (2022). Global shipping emissions in S5P/TROPOMI data. *EGU General Assembly*, *2022*. Vienna, Austria, 23–27 May 2022, EGU22-1795. https://doi.org/10.5194/egusphere-egu22-1795

Marmer, E., Dentener, F., Aardenne, J. v., Cavalli, F., Vignati, E., Velchev, K., et al. (2009). What can we learn about ship emission inventories from measurements of air pollutants over the Mediterranean Sea? *Atmospheric Chemistry and Physics*, *9*(18), 6815–6831. https://doi.org/10.5194/acp-9-6815-2009

Raupach, M. R., Marland, G., Ciais, P., LeQuéré, C., Canadell, J. G., Klepper, G., & Field, C. B. (2007). Global and regional drivers of accelerating CO_2 emissions. *Proceedings of the National Academy of Sciences of the United States of America*, *104*(24), 10288–10293. https://doi.org/10.1073/pnas.0700609104

Richter, A. (2009). Nitrogen oxides in the troposphere—What have we learned from satellite measurements? *European Physics Journal Conference*, *1*, 149–156. https://doi.org/10.1140/epjconf/e2009-00916-9

Riess, T. C. V. W., Boersma, K. F., van Vliet, J., Peters, W., Sneep, M., Eskes, H., & van Geffen, J. (2022). Improved monitoring of shipping NO2 with TROPOMI: Decreasing NOx emissions in European seas during the COVID-19 pandemic. *Atmospheric Measurement Techniques*, *15*(5), 1415–1438. https://doi.org/10.5194/amt-15-1415-2022

Schnurr, R. E. J., & Walker, T. R. (2019). Marine transportation and energy use. *Reference Module in Earth Systems and Environmental Sciences*, *2019*. https://doi.org/10.1016/B978-0-12-409548-9.09270-8

Smith, T. W. P., Jalkanen, J. P., Anderson, B. A., Corbett, J. J., Faber, J., Hanayama, S., et al. (2014). *Third IMO greenhouse gas study 2014*. International Maritime Organization (IMO). Vol. 327, Retrieved from https://docs.imo.org (last accessed on May 22, 2024).

UNCTAD (2022). Review of maritime transport, UNCTAD, Retrieved from https://unctad.org/pub;ication/review-maritime-transport-2022, (last accessed on May 22, 2024).

van Geffen, J., Eskes, H., Compernolle, S., Pinardi, G., Verhoelst, T., Lambert, J.-C., et al. (2022). Sentinel-5P TROPOMI NO_2 retrieval: Impact of version v2.2 improvements and comparisons with OMI and ground-based data. *Atmospheric Measurement Techniques*, *15*(7), 2037–2060. https://doi.org/10.5194/amt-15-2037-2022

Veefkind, J. P., Aben, I., McMullan, K., Förster, H., de Vries, J., Otter, G., et al. (2012). TROPOMI on the esa sentinel-5 precursor: A gmes mission for global observations of the atmospheric composition for climate, air quality and ozone layer applications. *Remote Sensing of Environment*, *120*, 70–83. https://doi.org/10.1016/j.rse.2011.09.027

Vinken, G. C. M., Boersma, K. F., van Donkelaar, A., & Zhang, L. (2014). Constraints on ship NOx emissions in Europe using GEOS-Chem and OMI satellite NO_2 observations. *Atmospheric Chemistry and Physics*, *14*(3), 1353–1369. https://doi.org/10.5194/acp-14-1353-2014